SCIENCE DU SOL n° 1985-1 - pp. 11-22 - PLAISIR-FRANCE

EXPERIMENTAL RESULTS ON SOIL MOISTURE CORRELATION WITH THERMAL INFRA-RED DATA

S.R.J. AXELSSON[1] and B.A. LUNDÉN[2]

ABSTRACT

In order to evaluate aerial thermography for soil moisture mapping, an agricultural area in central Sweden was thermally imaged one early afternoon and the following night. Soil samples, taken on 80 places spread over the area, were analysed with respect to volumetric water content, grain size distribution, porosity and organic material. Aluminium plates were put out at the sampling places, to make it possible to locate the sites in the thermal images.

The analysis of the relationship between thermal image data and soil data showed a significant correlation between soil moisture and temperature in both the daytime and the nighttime imagery. The accuracy increased considerably with the addition of meteorological data and soil type information to the interpretation procedure. (3)

INTRODUCTION

Today it is about ten years since the first results were presented on the use of IR thermography for soil water estimation (Idso *et al.*, 1975). The initial experimental studies were carried out using ground-based measurements, but very soon airborne thermal scanner data were incorporated (e.g. REGINATO *et al.*, 1976, SCHMUGGE *et al.*, 1978, CIHLAR *et al.*, 1979, HEILMAN and MOORE 1980, VLCEK and KING 1983).

Early the combined use of day and night temperature data was identified as a method for thermal inertia mapping. POHN, OFFIELD and WATSON (1974) applied this technique to generate thermal inertia maps for part of Oman in the Arabian Peninsula using data from the Nimbus satellites. WATSON (1975) had earlier developed a simulation model which was used at the interpretation. His model was later refined by KAHLE (1977), PRICE (1977), ROSEMA *et al.* (1978), PRATT *et al.* (1979) and AXELSSON (1977, 1980 and 1983).

In a Swedish study, LUNDÉN (1977) emphasized the needs of mathematical models for quantitative interpretation of thermal IR imagery. At the same time, AXELSSON (1977) developed an improved Fourier model for predictions of the surface temperature of bare surfaces. Later on (AXELSSON, 1980 and 1983), the potential accuracy of the technique and possible improvements using calibration surfaces were studied theoretically. Small-scale ground-based measurements in order to verify the modeling approach were also performed.

This paper presents the results of a more large scale experiment over an agricultural area characterized by great variations in soil type and water content. A main object of the experiment was to further investigate how the correlation between thermal data and soil water content in influenced by variations in soil composition and porosity.

1. Department of Electrical Engineering, University of Linköping, S-581 83 Linköping, Sweden.

2. Department of Physical Geography, University of Stockholm, S-106 91 Stockholm, Sweden.

3. This project was financially supported by the Swedish Board for Space Activities.

I. EXPERIMENTAL PROCEDURES

The experiment was carried out at the end of April 1984 in an agricultural area 20 miles north of Stockholm. The test area was characterized by bare fields with great differences in soil moisture content due to variations in topography and soil type. The airborne mission was composed of one flight in the early afternoon, at 13:20 (true solar time), and another one after midnight (01:20). During both flights, thermal IR line scanner data (8-13 micrometers) were obtained with a 2.5 milliradian sensor from an altitude of 600 m. In addition, black-and-white IR photographs were also obtained during the daytime flight. The weather during the mission day was characterized by clear sky and low wind speed. Weather data for the mission day and the days before were recorded at a meteorological station, put up in the area for this occasion.

The main purpose of the aerial photography was to obtain data over ground surface reflectance, an important parameter for the thermal modeling. Albedo was also measured in the field, with a hand-held radiometer (0.4-1.1 μm), for each of the soil sampling sites. In the mathematical models presented in the sequel, the radiometer data are used and no comparison has hitherto been done with data from the aerial photographs.

In the test area soil samples (0-5 cm) were collected in cylindrical metal containers at 80 sites. Three samples, chosen to minimize microtopographical effects, were taken at each site. At nine of the sites, samples were taken also from the top centimeter. The sampling was carried out during the afternoon of the mission day and should, according to earlier investigations (DANFORS *et al.*, 1977), be representative also for the conditions during the night flight. The soil samples were analysed in laboratory with respect to volumetric water content, organic matter content, grain size distribution (Figure 1) and porosity.

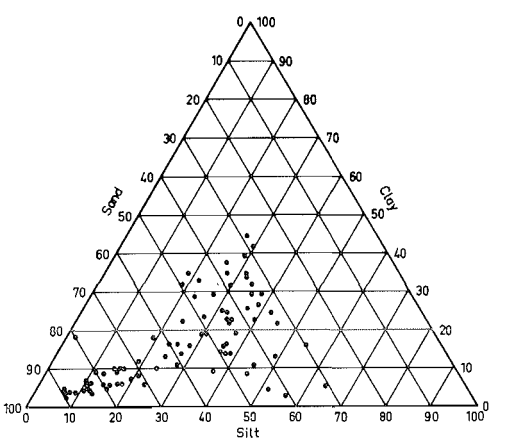

Figure 1 : Triangular soil classification chart showing the results (per cent by weight) of the mechanical analysis for the soils from the 80 samplings sites.
Triangle indiquant les textures des 80 échantillons.

For an evaluation of the radiation temperatures of the sampling sites, it must be possible to locate the sites in the thermal image. In order to solve that problem, aluminium plates (0.5 × 1.0 m large and 0.15 mm thick) had been put out at the 80 sampling places. Because of their extremely low emissivity (< 0.10), the plates functioned as reflectors of the cold sky radiation, and they therefore look like spots in the thermal imagery (Figure 2).

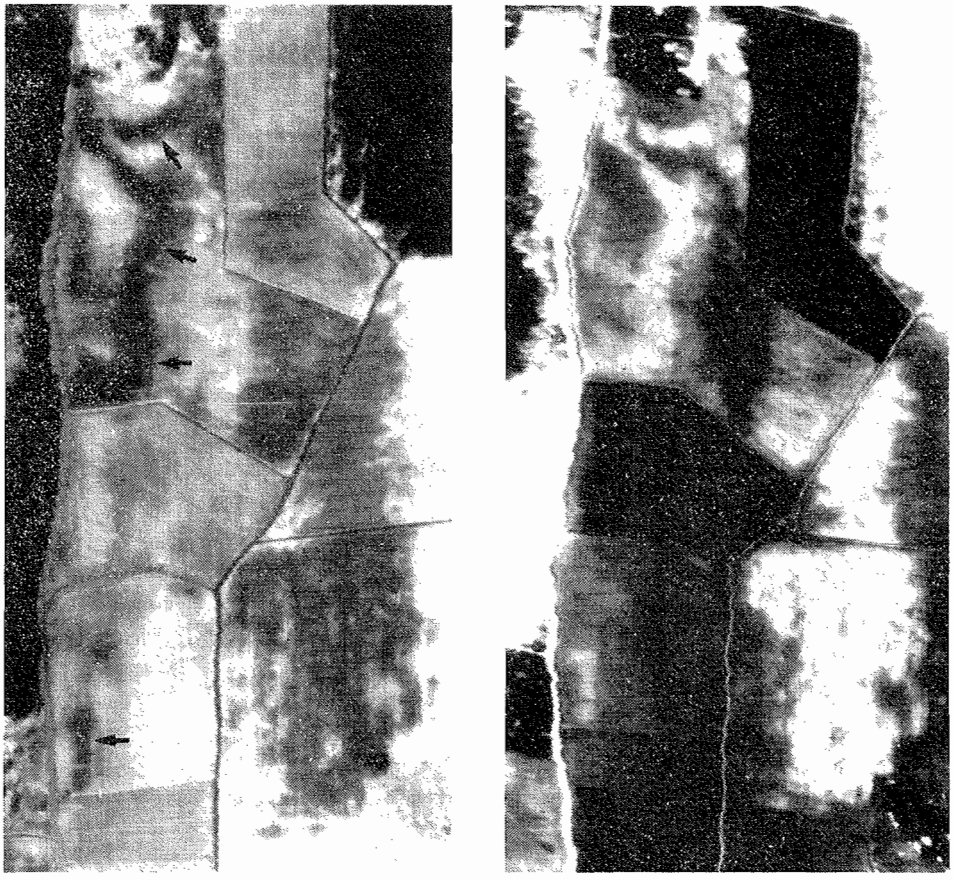

Figure 2 : Thermal images from the airborne mission over the test area, afternoon (left) and night (right). The images cover an area about 300 × 700 meters. Bright areas are warmer than dark ones ; the temperature interval for the daytime image is + 39° C to + 3° C and for the nighttime image 0° C to — 8° C. The coldest areas in the daytime image are tree-tops and the warmest are dry parts of the bare fields. In the nighttime image, clearings and fields with a dense grass cover are the coldest, and tree-tops are the warmest.

An area influenced by groundwater flow is marked with arrows in the daytime image. Due to temperature influence from the groundwater, sampling sites within this area gave anomalous data and were excluded from the analysis.

In the bare fields the aluminium plates, used to locate the sampling sites, can be seen as small cold spots.

Figure 2 : Images thermiques de la zone test (300 × 700 m), prises par avion, l'après-midi (gauche) et la nuit (droite). En blanc, les surfaces chaudes, en noir les froides. La température de brillance varie de + 3 à + 39° le jour et de 0° à — 8° la nuit. Le jour, les sols nus secs sont les plus chauds. La nuit, les défrichements et les sols couverts de végétation herbacée dense sont les plus froids.

Sur l'image de jour, les flèches indiquent l'influence de la nappe. Les zones correspondantes sont exclues de l'analyse. Les plaques d'aluminium servant de références, disposées dans les sols nus, apparaissent comme des petites taches froides (alignées).

For analysis, the thermal scanner data recorded during the flights were digitized and displayed on an image processing system. As the lower and upper scanner reference signals were also digitized, apparent temperature values could be obtained. With a software-controlled cursor and known distance from aluminium plates to sampling sites a 2 meters square was positioned over each site, and the mean apparent temperature was computed for pixels within the rectangle. The same procedure was repeated for all sites of both afternoon and nighttime imagery. With the software in the image processing system, it is possible to make corrections for emissivity variations and sky radiation. The thermal radiation of the ground also contains a reflected component from the sky. Its magnitude depends on the emissivity of the ground surface and the temperature of the sky. An emissivity value of 0.96 was chosen for all sampling sites and the sky temperature was measured with a hand-held infrared thermometer to 260 K for the afternoon and 250 K for the night. The corrected temperatures were then used in the correlation analysis.

The relationship between measured data and the soil characteristics were analysed at different steps of complexity. First, the unprocessed thermal IR and albedo data were correlated to volumetric soil moisture content. Secondly, the diurnal surface temperature amplitude, mean surface temperature, net radiation and latent heat flux were estimated from the measured thermal IR, albedo and meteorological data. These factors were identified as potential soil moisture indicators because of their strong coupling to evaporation and thermal inertia. At the third step, finally, the soil moisture contents were correlated to the thermal inertia (P) and the actual to potential evaporation ratio (M).

At the analysis seven sampling sites were excluded, which represented a thermal anomaly due to groundwater flow close to the surface (cf. Figure 2).

II. RAW DATA CORRELATION

The measured soil moisture of the 73 sampling sites were first compared with the albedo and the day/night temperatures. As a comparison the correlation with the diurnal temperature amplitude

$$\Delta T = T_{DAY} - T_{NIGHT} \qquad (1)$$

and the average temperature

$$\bar{T} = (T_{DAY} + T_{NIGHT})/2 \qquad (2)$$

were also computed. As shown by the results of Table I, there is a correlation between soil water content and the day temperature ($\rho = -0.62$), somewhat higher for the night temperature ($\rho = 0.69$) and a further improvement for the albedo data ($\rho = -0.75$). The correlation with the diurnal temperature amplitude (ΔT) is -0.66 and somewhat lower for the mean temperature ($\rho = -0.55$).

Table I : Correlation between volumetric soil moisture content (0-5 cm) and measured albedo (reflectance in 0.4-1.1 μm), day and night temperatures, diurnal temperature amplitude and average temperature (n = 73).

Tab. I : Corrélation entre l'humidité volumique (0-5 cm), l'albedo A (entre 0,4 et 1,1 μm), les températures de brillance de jour T_D et les températures de brillance de nuit T_N, l'amplitude diurne ΔT et la température IR moyenne $\bar{T}$ (73 échantillons).

Parameter	A	T_D	T_N	ΔT	$\bar{T}$
Correlation with soil moisture	— 0,75	— 0,62	0,69	— 0,66	— 0,55

The moderate coupling between soil moisture and the thermal data is due to the influence of various interfering factors. As shown by the correlation matrix of Table II, the day/night temperatures are related to the humus content and albedo. It should also be noticed that there is a strong relation between water content and the humus content of the soil ($\rho = 0.92$). The correlation with sand and clay contents is fairly low, however.

1) Albedo influence

A significantly high correlation was obtained between albedo and soil moisture (Table I). There are several reasons for this effect. The most obvious one is caused by the reduced reflectance of a wet surface compared to a dry one. There is also an albedo dependence on the soil content of organic material ($\rho = -0.71$). For the soils in the test area, there was furthermore a strong correlation between humus content and soil moisture ($\rho = 0.92$). Consequently, sampling sites with high albedo represent soils with low humus and water contents, while areas with low albedo are representative to humus-rich samples with high soil moisture. These combined effects contribute to the enhanced relationship between water content and albedo.

Table II : Correlation matrix (n = 73)

Matrice de correlation

T_D = **Day IR-temperature** — **POR = Porosity** *(porosité)*

T_N = **Night IR-temperature** — **HC = Humus content** *(matière organique)*

A = Reflectance in 0.4-1.1 μm — **CC = Clay content** *(argile)*

WC = Water content (0-5 cm) *(humidité)* — **SC = Sand content** *(sable)*

	T_D	T_N	A	WC	POR	HC	CC	SC
T_D	1.00	— 0.80	0.46	— 0.62	— 0.32	— 0.53	0.04	0.16
T_N	— 0.80	1.00	— 0.61	0.69	0.42	0.66	— 0.23	0.04
A	0.46	— 0.61	1.00	— 0.75	— 0.70	— 0.71	— 0.28	0.47
WC	— 0.62	0.69	— 0.75	1.00	0.79	0.92	0.24	— 0.50
POR	— 0.32	0.42	— 0.70	0.79	1.00	0.87	0,27	— 0.57
HC	— 0.53	0.66	— 0.71	0.92	0.87	1.00	0.09	— 0.45
CC	0.04	— 0.23	— 0.28	0.24	0.27	0.09	1.00	— 0.73
SC	0.16	0.04	0.47	— 0,50	— 0.57	— 0.45	— 0.73	1.00

2) Influence of humus content

The soil samples showed a great variation in humus content. In order to investigate how this effect influences the accuracy, the data were divided into two sub-sets :

A. Soil samples with a humus content by weight higher than 10 per cent (n = 35).

B. Soil samples with humus content lower than 10 per cent (n = 39).

The results of Table III show a significantly improved correlation between soil moisture and thermal data for the humus-rich soil samples.

Table III : Correlation between volumetric water content (0-5 cm) and raw data for two different sub-sets with high and low humus contents (HC) respectively.

Tab. III : Corrélation entre l'albedo, les températures de brillance et l'humidité (0-5 cm) pour 2 lots constitués à partir du taux de matière organique.

PARAMETER (see Table I)	SOIL MOISTURE CORRELATION All (n = 73)	HC ⩾ 0.1 (n = 35)	HC ⩽ 0.1 (n = 39)
A	— 0.75	— 0.50	— 0.47
T_N	— 0.62	— 0.76	— 0.34
T_D	0.69	0.84	0.02
ΔT	— 0.66	— 0.80	— 0.31
$\overline{T}$	— 0.55	— 0.67	— 0.37

The set with low humus content showed a weaker response. In particular, the night temperature correlation drops to a very low value (ρ = 0.02). As expected the albedo showed a reduced correlation for both sub-sets (ρ = 0.50 and — 0.47) compared to the correlation of all the 73 samples.

3) Influence of sand content

The influence of the sand content upon the correlation between moisture and the measured thermal IR-temperature was also analysed. As shown by the results in Table IV, the correlation between soil moisture and the thermal data increases significantly when samples with the highest sand contents are excluded. When the sand content is lower than 0.40, the correlation between soil moisture and the day temperature changes from — 0.62 to — 0.91. The night temperature correlation is increased from 0.69 to 0.88. Also the correlation of the temperature amplitude (ΔT) and the mean temperature ($\overline{T}$) improve with decreased sand content. The soil moisture correlation with respect to ΔT increases to — 0.92 for the sub-set with sand content lower than 40 %.

Table IV : Correlation between volumetric water content and raw data for varying sand content (SC)

Tab. IV. : Corrélation entre les températures de brillance et l'humidité (0-5 cm) pour 3 lots constitués à partir de la teneur en sable.

PARAMETER (see Table I)	SOIL MOISTURE CORRELATION All (n = 73)	SC ⩾ 0.60 (n = 26)	SC ⩽ 0.60 (n = 48)	SC < 0.40 (n = 19)
A	— 0.75	— 0.64	— 0.70	— 0.47
T_D	— 0.62	— 0.35	— 0.81	— 0.91
T_N	0.69	0.71	0.83	0.88
ΔT	— 0.66	— 0.43	— 0.83	— 0.92
$\overline{T}$	— 0.55	— 0.26	— 0.76	— 0.88

III. CORRELATION WITH NET RADIATION AND LATENT HEAT FLOW

1) Basic relationships

In the preceding section, the soil moisture correlation of albedo and thermal raw data were studied. Furthermore, the day — night temperature difference (ΔT) and mean temperature ($\overline{T}$) were also investigated. An important question is whether there are some other parameters, which are sensitive to the water content and can be simply derived from the thermal and albedo raw data.

One such soil moisture indicator is the net radiation (Rn), which is indirectly related to soil moisture through albedo (A) and surface temperature (T) :

$$Rn = I\,(1 - A) + \sigma\,\varepsilon\,(T^4_{SKY} - T^4) \qquad (3)$$

where I is the incident sun radiation, T_{SKY} is the black-body temperature of the long-wave sky radiation, ε is the emissivity and σ is the Stefan-Bolzmann constant.

From the heat balance equation, we can also express the net radiation as

$$Rn = H + LE + Q_O \qquad (4)$$

where H is sensible heat flux, LE is the latent heat flux due to evaporation, and Q_O is the downward soil heat flux.

The sensible heat flux is proportional to the surface-to-air temperature difference :

$$H = h\,(T - T_a) \qquad (5)$$

The factor h in (5) is strongly related to wind-speed, but also surface roughness, and stability conditions of the lower atmosphere have significant effects (BUSINGER *et al.*, 1971).

In Eq. (4), an increase of LE and Q_O might be expected when soil-moisture increases due to enhanced evaporation and thermal conductivity of the soil layer. The sum of these two components is from (4) :

$$G = LE + Q_O = Rn - H \qquad (6)$$

In particular, if diurnal mean values are considered, $\overline{Q_O}$ is usually much smaller than the other mean fluxes of (4) and (6). This means $\overline{G} \approx \overline{LE}$, and

$$\overline{LE} \approx \overline{Rn} - \overline{H} \qquad (7)$$

At the analysis of the experimental data, both the net radiation at the day measurement (Rn_d) and the day-night mean value ($\overline{Rn}$) were computed from Eq. (3) with surface temperature (T), albedo (A), and incident (radiation (I and T_{SKY}) as input. From Eqs. (6) — (7), $\overline{LE}$ and G_d (i. e. the day value of G) were also derived using estimates of the sensible heat flux (H) and net radiation (Rn).

Table V : Soil moisture correlation of raw data and processed data (n = 73)

Corrélation entre l'humidité des sols pour des données brutes et des données traitées.

Parameter	T_D	T_N	A	ΔT	T	$\overline{Rn}$	$\overline{LE}$	Rn_d	G_d
Soil moisture correlation	—	0,62	0,69	— 0,75	— 0,66	— 0,55	0,81	0,75	0,81	0,80

2) Results

As shown by Table V, the correlation between soil water content and the processed data $\overline{Rn}$, $\overline{LE}$, Rn_d, and G_d is highly improved compared to the correlation with the thermal raw data. The correlation of $\overline{Rn}$, Rn_d and G_d are all of the order of 0.8 compared to 0.69 and — 0.62 for the night and day temperatures. The influence of humus/sand contents will be further discussed in the next section.

IV. THERMAL INERTIA AND EVAPORATION INDEX

1) Introduction

The day and night temperatures as well as net radiation and evaporation depend upon both soil characteristics and the meteorological conditions at the time of acquisition. Some improvements of the results of the data analysis might be achieved, if we succeed in determining parameters, which are more uniquely related to the soil factors. This was the basic ideas of the thermal inertia approach (Watson, 1975, Kahle 1977, Price 1977, Rosema *et al.* 1978, Pratt 1979, Axelsson 1980 and 1983). By definition the thermal inertia is related to the thermal conductivity (λ) and capacity (C) of the soil layer according to

$$P = \sqrt{\lambda C} \qquad (8)$$

Besides a strong dependence on the soil water content, the thermal inertia is also influenced by the mineral composition and porosity.

Another parameter to be used below is the evaporation index ($0 \leqslant M \leqslant 1$), which is defined as the actual to potential evaporation rate at the same surface temperature. Obviously this parameter should be highly related to the water content close to the soil surface.

At the data analysis the day/night temperatures of the sampling sites are translated into thermal inertia (P) and evaporation index (M) using a mathematical model which is calibrated from meteorological data during 96 hours before the time of acquisition. From the derived P— and M—values, the correlation with soil moisture is finally computed and compared.

2) Thermal modeling

The surface temperature of a bare soil surface is controlled by the heat transfer at the surface boundary. If a one-dimensional model is assumed, the temperature T (x,t) and heat flow Q (x,t) are determined by

$$\left.\begin{aligned} Q &= -\lambda \frac{\delta T}{\delta x} \\ \frac{\delta Q}{\delta x} &= -\frac{d}{dt}(CT) \end{aligned}\right\} \qquad (9)$$

where t is time, x is depth, λ is the thermal conductivity, and C is the heat capacity per unit volume.

The boundary condition at the surface is determined from Eq. (4)

$$Q_0 = -\lambda \left.\frac{\delta T}{\delta x}\right|_{x=0} = Rn - H - LE \qquad (10)$$

3) Finite difference model

The surface temperature can be computed from Eqs. (9) and (10) using the method of finite difference (Kahle 1977). The upper ground layer is then subdivided into thin horizontal slices. Before the computer processing starts, the initial temperatures and the parameters involved have to be defined. Temperatures and heat fluxes at time $t = (m + 1)\ \triangle t$ are updated using the heat balance of Eq. (10).

4) Interpretation algorithms

At the interpretation, tables of day and night temperatures of the ground surface were computed as a function of albedo, thermal inertia and evaporation index using as input meteorological data from the test site during a four-day period before the acquisition of the thermal data. From the measured thermal IR-temperatures (day and night) and albedo estimates, the thermal inertia and evaporation index were determined using the inverted tables.

5) Results

The results of the computer processing (Table VI) show a significant correlation between soil moisture and the thermal inertia (P) and evaporation index (M) when all the soil samples are considered ($\varrho = 0.72$ and 0.74). These values are higher than the correlation of the thermal raw data. However, a still higher correlation was obtained using the average latent heat ($\overline{LE}$), net radiation ($\overline{Rn}_d$ and Rn), or G_d, see Eq. (6), as soil moisture indicators.

Table VI : Correlation with volumetric soil moisture content (0-5 cm) for all samples and two sub-sets with different humus content (HC).

Tab. VI : Corrélation entre divers paramètres et l'humidité (0-5 cm) pour 2 lots constitués à partir du taux de matière organique.

PARAMETER (see text)	SOIL MOISTURE CORRELATION All (n = 73)	HC ⩾ 0.1 (n = 35)	HC ⩽ 0.1 (n = 39)
T_D	— 0.62	— 0.76	— 0.34
T_N	0.69	0.84	0.02
A	— 0.75	— 0.50	— 0.47
$\triangle T$	— 0.66	— 0.78	— 0.31
$\overline{T}$	— 0.55	— 0.67	— 0.37
$\overline{Rn}$	0.81	0.65	0.59
$\overline{LE}$	0.75	0.70	0.53
Rn_d	0.81	0.66	0.55
G_d	0.80	0.74	0.54
M	0.72	0.70	0.50
P	0.74	0.83	0.26

When two sub-sets with different humus content are formed, the results are changed. The correlation of $\overline{Rn}$, $\overline{LE}$, Rn_d, G_d, A and M are then somewhat reduced. The other parameters show an increased soil moisture correlation for humus contents $\geqslant 0.10$, while a significant drop occurs for the low-humus set (HC $\leqslant 0.10$).

The results improve further, if instead the samples are divided into sets with varying sand contents (Table VII). For a sand content less than 60 % (48 of 73 samples), the soil moisture correlation of both the thermal inertia (P) and evaporation index (M) exceed the 80 % level and for SC $<$ 40 %, the correlation coefficient of P reaches the 90 % level. Correlation coefficients of the same order are also obtained for the day and night temperatures and most of the other processed thermal data.

Looking at the set of samples with a sand content higher than 60 %, the correlation coefficients decrease in general. An obvious correlation ($\rho \geqslant 0.64$) is still preserved for T_N, $\overline{Rn}$, Rn_d, G_d and P, however.

The soil water contents discussed above represent samples from 0-5cm. Comparison with the nine soil samples from 0-1 cm showed improved correlation, but due to the limited number no further conclusions are drawn.

It should be noticed that the albedo correlation to soil moisture is decreased for all the sub-sets in Table VI and VII.

Table VII : Correlation with volumetric soil moisture content (0-5 cm) for varying sand content (SC)

Tab. VII : Corrélation entre divers paramètres et l'humidité (0-5cm) pour 3 lots constitués à partir de la teneur en sable.

PARAMETER (see text)	SOIL MOISTURE CORRELATION All (n = 73)	SC $\geqslant$ 0.60 (n = 26)	SC $\leqslant$ 0.60 (n = 48)	SC $<$ 0.40 (n = 19)
T_D	— 0.62	— 0.35	— 0.81	— 0.91
T_N	0.69	0.71	0.83	0.88
A	— 0.75	— 0.64	— 0.70	— 0.47
ΔT	— 0.66	— 0.43	— 0.83	— 0.92
$\overline{T}$	— 0.55	— 0.26	— 0.76	— 0.88
$\overline{Rn}$	0.81	0.67	0.80	0.69
$\overline{LE}$	0.75	0.52	0.82	0.83
Rn_d	0.81	0.69	0.79	0.66
G_d	0.80	0.64	0.83	0.80
M	0.72	0.46	0.81	0.85
P	0.74	0.65	0.84	0.90

CONCLUSIONS

The soil moisture correlation with thermal IR data has been studied for an agricultural area with great variations in soil water content (9-60 per cent by volume) and soil composition (sand content, 29-90 per cent by weight, clay content, 2-44 per cent, and humus content, 1-37 per cent). In particular, the potential improvements with the addition of meteorological data and soil type information to the interpretation procedure were investigated.

The results of the analysis show that there is a definite correlation between the day and night temperatures and the soil water content ($\rho = -0.62$ and 0.69, respectively). Significant improvements are possible by using processed data like net radiation, evaporation and thermal inertia ($\rho = 0.72$-0.81).

A further increase of the soil moisture correlation (up to — 0.92) was obtained, when samples with low humus or high sand content were excluded at the analysis. The correlation values of the low-humus sub-set [HC $\leqslant$ 10 %) were reduced, however. In particular the night temperature correlation dropped to a very low value ($\rho = 0.02$), while the net radiation and the evaporation related parameters showed a more moderate reduction ($\rho = 0.50$-0.59).

An improved soil moisture correlation should be expected when meteorological data or soil type information are used at the interpretation, since the air temperature, wind speed and net radiation are factors which highly influence the surface temperature. Also the soil composition has an obvious effect upon thermal inertia, field capacity and diffusion resistance to water transport in the uppermost soil layer. The use of thermal inertia and evaporation index at the interpretation might also reduce the need for ground truth data in future applications. In order to further verify the consistency of the results, additional field experiments should be carried out at other soil water status and weather conditions.

RELATIONS ENTRE L'HUMIDITE DES SOLS ET LES DONNEES DE L'INFRA-ROUGE THERMIQUE : RESULTATS EXPERIMENTAUX

Afin d'évaluer l'importance de la thermographie aérienne lors d'un relevé de l'humidité du sol, une zone agricole du centre de la Suède a été étudiée successivement durant un après -midi et la nuit suivante. Des échantillons de sol ont été prélevés dans 80 sites de la zone étudiée et ont été analysés pour déterminer le volume d'eau, la répartition des éléments granulométriques (figure 1), la porosité et le taux de matière organique. Des plaques d'aluminium ont été placées aux endroits où ont été prélevés les échantillons, cela afin de permettre de les localiser sur les images thermiques (figure 2).

L'analyse de la relation entre les données des images thermiques et celles provenant de l'analyse du sol a mis en évidence une corrélation significative entre l'humidité du sol et la température de l'air, tant le jour que la nuit. La précision des résultats augmente considérablement quand on prend en compte dans l'analyse les données météorologiques et les caractéristiques sur la nature du sol (tab. I à VII).

REFERENCES

AXELSSON SRJ., 1977. — Model for the estimation of surface temperature of homogenous half-spaces at periodic heating. (In Swedish). Saab-Scania, Technical Report RL-0-3B445, 6 p.

AXELSSON S.R.J., 1980. — On the accuracy of thermal inertia mapping by infrared imagery. Proc. 14th Int. Symp. Rem. Sens. Env., pp. 359-378.

AXELSSON S.R.J., 1983 — Improved calibration algorithms for thermal IR mapping- Proc. 16th Int. Symp. Rem. Sens. Env., pp. 771-784.

BUSINGER J.A., WYNGAARD J.C., ZZUMI Y. and BRADLEY E.F., 1971. — Fluxprofile relationships in the atmospheric surface layer. Journal Atmospherical Science 28, pp. 181-189.

CIHLAR J., SOMMERFELDT T. and PATERSON B., 1979. — Soil water content estimation of fallow fields from airborne thermal scanner measurements. Canadian Journal of Remote Sensing 5, pp. 18-32.

DANFORS E., LUNDÉN B., SVENSSON K. and WASTENSON L., 1977. — Markvattenkartering medelst IR-termografi. Summary : Soil water mapping by means of infrared thermographic technique. Meddelande 3:22A, Inst. för kulturteknik, Tekniska Högskolan, Stockholm, 63 p.

HEILMAN J.L. and MOORE D.G., 1980. — Thermography for estimating nearsurface soil moisture under developing crops. Journal of Applied Meteorology 19, pp. 324-328.

IDSO S.B., SCHMUGGE T.J., JACKSON R.D. and REGINATO R.J., 1975. — The utility of fallow fields from airborne thermal scanner measurements. Canadian Journal Journal Geophysical Research 80, pp. 3044-3049.

KAHLE A.B., 1977. — A simple model of the earth's surface for geologic mapping by remote sensing. Journal Geophysical Research 82, pp. 1673-1680.

LUNDÉN B., 1977. — Infrarödtermografi för markvattenstudier. Summary : IR-thermography as a means of studying soil water distribution. Forskningsrapport 25, Naturgeografiska institutionen, Stockholms universitet, 60 p.

POHN H.A., OFFIELD T.W. and WATSON K., 1974. — Thermal inertia mapping from satellite. Discrimination of geologic units in Oman. Journal Research U.S. Geol. Survey 2, pp. 147-158.

PRATT D.A. and ELLYETT C.D., 1979. — The thermal inertia approach to mapping of soil moisture and geology. Remote Sensing of Environment 8, pp. 151-168.

PRICE J.G., 1977. — Thermal inertia mapping : A new view of the Earth. Journal Geophysical Research 82, pp. 2582-2590.

REGINATO R.J., IDSO S.B., VEDDER J.F., JACKSON R.D., BLANCHARD M.B. and GOETTELMAN J., 1976. — Soil water content and evaporation determination by thermal parameters obtained from groundbased and remote measurements. Journal Geophysical Research 81, pp. 1617-1620.

ROSEMA A., BIJLEVELD J.H., REINEGER P., TASSONE G., BLYTH K. and GURNEY R.J., 1978. — TELL-US. A combined surface temperature, soil moisture and evaporation mapping approach. Proc. 12 th Int. Symp. Rem. Sens. Env., pp. 2267-2276.

SCHMUGGE T., BLANCHARD B., ANDERSON A. and WANG J., 1978. — Soil moisture sensing with aircraft observations of the diurnal range of surface temperature. Water Resources Bulletin 14, pp. 169-172.

VLCEK J. and KING D., 1983. — Detection of subsurface soil moisture by thermal sensing : Results of laboratory, close-range and aerial studies. Photogrammetric Engineering and Remote Sensing 49, pp. 1593-1597.

WATSON K., 1975. — Geologic applications of thermal infrared images. Proc. IEEE 63, pp. 128-137.